IONOPHORE PROPERTIES OF A SYNTHETIC ALPHA-HELICAL TRANSMEMBRANE FRAGMENT OF THE MITOCHONDRIAL H^+ ATP SYNTHETASE OF *SACCHAROMYCES CEREVISIAE*

Comparison with Alamethicin

G. MOLLE,* J. Y. DUGAST,* H. DUCLOHIER,* P. DAUMAS,‡ F. HEITZ,‡ AND G. SPACH*
Polymères, Biopolymères et Membranes, UA 500 Centre National de la Recherche Scientifique, (CNRS) B.P. 67, Faculté des Sciences, 76130 Mont-Saint-Aignan, and ‡Physico-Chimie des Systèmes Polyphasés, UA 330 CNRS B.P. 5051, 34033 Montpellier Cedex, France

ABSTRACT A 22-amino acid polypeptide was synthesized to model the central transmembrane segment of subunit 8 of the H^+ ATP synthetase of *Saccharomyces cerevisiae* and to test ionophore properties. Solid-phase synthesis was conducted on benzhydrilamino resin, and purification followed by high pressure liquid chromatography allowed the isolation of the pure product whose NH_2 terminal was acetylated and whose molecular weight determined by Fast Atomic Bombardment was the expected 2,666. The infrared spectrum of this peptide in the solid state reveals a fully α-helical conformation, whereas in low dielectric constant solvents the α-helical content is 60%, as determined by circular dichroism studies. Macroscopic current–voltage curves displayed by different planar lipid bilayers (monomyristoleoyl-glycerol and phosphatidylethanolamine) doped with this peptide suggest a weakly voltage-dependent conductance. Only one conductance level is observed in any given single-channel conductance experiment. However, a series of experiments shows a distribution of conductance states, most often 440 or 3,000 pS, and occasionally 80, 1,200, or 6,500 pS. This behavior contrasts with the usual behavior of alamethicin, chosen as a model of "aggregating-helices" ionophore and whose conductance fluctuates continually between substates, through uptake and release of monomers. Nevertheless, alamethicin too can display, under certain conditions, long-lived and mono-level conductance states similar to those reported here for the newly synthesized peptide. These properties could possibly be explained by the formation of large domains of helical rods with a set of allowed and independent ionic pathways.

INTRODUCTION

Some of the best-known channels of natural excitable membranes, i.e., the sodium and voltage-dependent channel, and the acetylcholine-mediated channel, now seem to be composed of many transmembrane α-helices and the aligned hydrophilic amino acids of a few helices at the core of the channel would form the ionic pathway (1–4). Since a similar hydropathy profile has also been found for the transmembrane fragments of another important and recently sequenced channel, the gap junction (5, 6), the possibility exists that the various ionic channels might be built, at least at the level of secondary structure, according to a common design (see reference 7). Although little is known about their tertiary structure, one of the main distinctive features of these channels is the number of subunits involved together with their different selectivity and conductance levels. Therefore, the study of model ionic channels, functioning through aggregation of monomers, and the "barrel-stave" scheme initially proposed for alamethicin (8, 9) and refined recently (10, 11), seem to merit further consideration. Another opportunity to test such a mechanism is offered by a 48-amino acid polypeptide (Fig. 1 *A*), subunit 8 of the F_0 part of the H^+ ATP synthetase from *Saccharomyces cerevisiae,* recently isolated and sequenced (12). This subunit, whose presence is essential for the H^+ ATPase activity (proton translocation carried out by subunit 9 [13]), displays a central hydrophobic segment of about 20 amino acids thought to be, through secondary structure predictions, an α-helix spanning the membrane. In this segment, the two most hydrophilic residues, Thr 22 and Gln 29, are nearly aligned (see the helix projection in Fig. 1 *B*). α-Helices aggregation and ionophore properties could be reasonably inferred (14), especially if one takes into account that the contact zones with lipids and other monomeric peptides are rich in Leu and Phe. This is supported by preliminary experiments showing channel activity, with the whole subunit 8

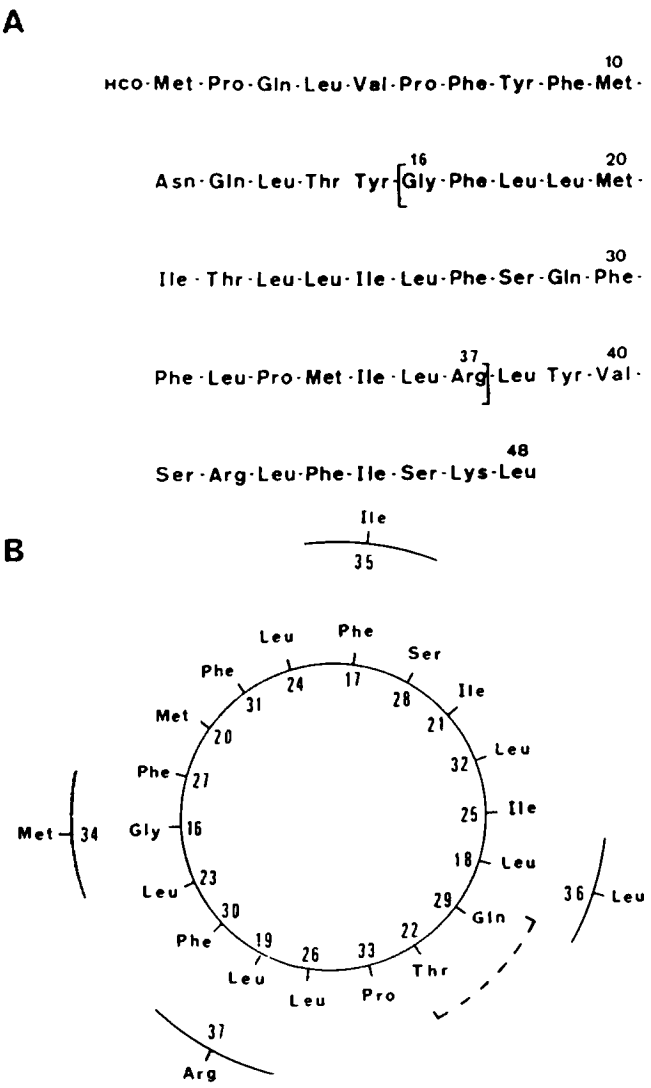

FIGURE 1 (*A*) Aminoacid sequence of subunit 8 isolated from the H^+-ATP-synthetase of yeast mitochondria. Vertical bars delineate the segment selected for synthesis. (*B*) Projection on a plane perpendicular to the axis of the α-helix assumed for the segment (16-37); the dotted line points out the hydrophilic sector (Thr 22-Gln 29).

extracted from the mitochondrial H^+ ATP synthetase (15). Here, we test this hypothesis with a synthetic peptide designed to reproduce the central segment 16-37, delineated by vertical bars on Fig. 1 *A*, and whose NH_2 terminus is acetylated and whose COOH terminus bears an amido group.

The synthesis and isolation procedures of this peptide, hereafter referred to as peptide 8(16-37) for the nonacetylated form and peptide 8(16-37)a for the acetylated form, are described together with conformational studies, suggesting a predominant α-helical structure in membranes. Macroscopic current–voltage curves point out a weakly voltage-dependent conductance. Single-channel experiments on planar lipid bilayers show that this peptide induces ionic channels with fixed conductance values, i.e., with no fluctuations between substates. We also present some results with alamethicin to compare ionophore properties between this reference molecule for aggregation-type channels and the newly synthesized peptide. This study suggests that some ionophores, including peptide 8(16-37)a and even alamethicin under certain conditions, could form in membranes large aggregates or domains with a set of "open" and independent configurations and whose size would prevent the uptake and release of monomers by the central conducting pore.

MATERIALS AND METHODS

Products and Apparatus

The solid-phase synthesis of the peptide was carried out on a semi-automatic synthesizer SAP IV from SEMPA-CHIMIE (Paris). Radioactivity was measured on a counter (1215 Rack Beta model; LKB Instruments, Inc., Gaithersburg, MD). The Fast Atomic Bombardment (FAB)[1] mass spectra were obtained on a ZAB HF model from VG Analytical (Manchester, UK) at the Service Central d'Analyses du CNRS in Lyon.

Thin layer chromatography (TLC) was performed on Silica gel 60 F 254 plates of size 5 × 20 cm and on RP 18 F 254 S plates of size 5 × 10 cm (E. Merck, Darmstadt, FRG). Chromatograms were developed with ninhydrin, vanilline, or Reindel and Hoppe reagent. The following solvent mixtures were routinely used: CH_2Cl_2/methanol (MeOH)/acetic acid (AcOH) (85:10:5), $CHCl_3$/MeOH/AcOH (82:13:5), ethylacetate (EtOAc)-pyridine (Pyr)/AcOH/H_2O (5:5:1:3).

High pressure liquid chromatography (HPLC) was performed on an LKB system: two pumps (2150 model), a 2152 solvent programmer, a Rheodyne Inc. (Cotati, CA) injector, and a 2151 tunable UV-VIS detector. An RP 8 spheri 5 (5 μm) column (from Brownlee Labs, Santa Clara, CA) and a C 18 TSK ODS 120 T (10 μm) column (from LKB Instruments, Inc.), both of 4.6 × 2.50-mm dimensions, were used for analytical chromatography. The latter type, but of dimensions 7.8 × 300 mm, was also used for semi-preparative chromatography. Solvents were mainly MeOH or EtOH (RS, HPLC; Farmitalia, Paris), H_2O (delivered from a Millipore Corp. [Bedford, MA] Q Water apparatus), and TFA (Fluka AG, Buchs, Switzerland).

For conformational studies, infrared spectra of the peptide in the solid state (from a dried MeOH or $CHCl_3$ film) were recorded on a 983 model (Perkin-Elmer Corp., Norwalk, CT), and circular dichroism measurements in low polarity media were performed on a Roussel-Jouan (Paris) Mark V dichrograph.

Preparation of Reagents

The *N*-α-*t*-butyloxycarbonyl (Boc) forms of those aminoacids not requiring protection of the lateral groups (Leu, Ile, Phe, Met, Pro) are synthesized in the laboratory, with di-*t*-butyldicarbonate [$(Boc)_2O$], and their purity is confirmed by TLC. *N*-Boc-L-nitroarginine, *N*-Boc-*O*-benzyl-L-threonine, *N*-Boc-*O*-benzyl-L-serine, and *N*-Boc-L-glutamine-*p*-nitrophenyl esters are BACHEM products (Bubendorf, Switzerland). *t*-Boc-glycine radio labeled with ^{14}C (2.6×10^5 cpm/mg) is prepared from ^{14}C-Gly (0.25 mCi) from New England Nuclear (Boston, MA). The solid-phase synthesis is performed on a benzhydrilamino resin reticulated with 1% divinylbenzene (UCB Bioproduct, Brussels, Belgium), whose

[1] *Abbreviations used in this paper:* AcOH, acetic acid. Boc, *t*-butyloxycarbonyl; $(Boc)_2O$, di-*t*-butyldicarbonate; DCC, *N-N'* dicyclohexyl carbodiimide; DIEA, di-isopropyl ethyl amine; DMF, dimethylformamide; EtOAc, ethylacetate; EtOH, ethanol; FAB, Fast Atomic Bombardment; HF2P, hexafluoroisopropanol; HOBT, *N*-hydroxybenzotriazole; HPLC, high pressure liquid chromatography; MeOH, methanol; MMG, monomyristoleoyl-glycerol; MPG, monopalmitoleoyl-glycerol; PE, phosphatidylethanolamine; TFA, trifluoroacetic acid; TLC, thin layer chromatography.

substitution extent was 0.62 mmol/g. Solvents (MeOH grade RPE ACS [Carlo Erba] and CH_2Cl_2 [Prolabo Rectapur]) are distilled twice before use. To remove all amines from dimethylformamide (DMF), it is heated under benzene reflux for 2 h on ninhydrine (2g/liter). After benzene elimination by azeotropic distillation, DMF is distilled under vacuum (60°C under 14 mm) and stocked in the dark on a molecular sieve. Trifluoroacetic acid (TFA) (98%), *N-N'*-dicyclohexyl carbodiimide (DCC), *N*-hydroxybenzotriazole (HOBT) (Fluka AG), and di-isopropyl ethyl amine (DIEA) (97%, Aldrich Chemical Co., Milwaukee, WI) are used without further purification.

Synthesis of Peptides 8(16-37) and 8(16-37)a

The solid-phase method (16) was used. In a 20-ml reactor are introduced 0.5 g of benzhydrilamino resin, 1 mmol of Boc-protected amino acid, HOBT, and DCC with 5 ml DMF and freshly distilled 5 ml CH_2Cl_2. Coupling is conducted for 2 h under shaking. After several washings with CH_2Cl_2 and MeOH, a Kaiser test allows estimation of the coupling yield. Amino acid coupling steps proved to be sometimes difficult, because several couplings had to be achieved and in most cases acetylations, with 30 μl AcOH + 0.5 mmol DCC, were necessary to block those NH_2 groups that remained free. When the Kaiser test is negative and before coupling the next amino acid, the amine function is deprotected by treatment of the resin with a solution of TFA (30% in CH_2Cl_2) containing 2% ethane dithiol. The resin is then neutralized by DIEA (10% in CH_2Cl_2), and washed alternatively with MeOH and with CH_2Cl_2. Glutamine coupling is carried out without DCC and with the activated ester (*O*-paranitrophenyl) in DMF alone. No chromophore group being present in the designed sequence, the last amino acid to be coupled (Gly 16) is enriched in ^{14}C to allow characterization of the expected product by radio β-counting.

Finally, 900 mg of peptidyl-resin are obtained, 400 mg of which are acetylated, as described above, on the NH_2 terminus. Elimination of all the groups protecting the lateral chains, and peptide separation from the resin, is realized in liquid hydrogen fluoride at 0°C for 1 h, with dimethyl sulfur and *p*-cresol as scavengers, leaving an amidated COOH-terminal peptide.

After extensive washings with diethyl oxide, the peptide is extracted by hexafluoroisopropanol (HF2P). The solution is diluted with H_2O and then lyophilized. 225 mg of the non-acetylated product and 141 mg of the acetylated one are obtained. The raw products are insoluble in water and only slightly soluble in usual organic solvents. Formic acid or HF2P had to be used to dissolve these peptides, which were purified by HPLC with $EtOH/H_2O$ gradients.

Macroscopic and Single-Channel Conductance Experiments

Black lipid membranes are formed on a 0.3-mm hole in a Teflon septum between two electrolyte solutions of unbuffered 1 M KCl, according to a procedure similar to the one described by Eisenberg et al. (17), except that only one pair of silver chloride electrodes is used. Membrane-forming solutions are either 1-monopalmitoleoyl-glycerol (Sigma Chemical Co., St. Louis, MO), referred to as MPG, or monomyristoleoyl (MMG; from NU-CHECK Prep. Inc.), both made to 2% in *n*-decane (Fluka AG), or bacterial (*E. coli*) phosphatidylethanolamine (PE; Sigma Chemical Co.) made to 1% in *n*-decane. Bilayer formation is monitored by capacitance from current–voltage responses and the relation $I_c = C(dV/dt)$. A high gain current amplifier (model 427, with rise time adjustable to 0.1–300 ms; Keithley Instruments, Inc., Cleveland, OH) is used to visualize the signals on an oscilloscope and send them either to an *X-Y* paper plotter or to a II E microcomputer (Apple Computer Inc., Cupertino, CA), according to which kind of experiment (macroscopic or single-channel conductance, respectively) is performed. For the macroscopic conductance experiments, the current–voltage curves are recorded by testing the membranes with a triangular sweep of voltage (up to ±200 mV, 35 s per cycle) and three to five runs are applied to check reproducibility. For the single-channel experiments, the computer (sampling time ranging from 0.2 to 500 ms), coupled to a printer, allows retrieval of current fluctuations and amplitude histograms. To reduce electrical and microphonic noises, the chamber and electrodes are enclosed in a shielded box on a concrete block resting on inflated innertubes.

In both kinds of experiments, the peptide is added only after checking silence and stability of bare membranes. A series of tests using voltages up to ±200 mV was conducted for ~30 min. The peptide 8(16-37)a stock solution is $2 \cdot 10^{-5}$ M in MeOH and the final concentration is in the range of 10^{-8}–10^{-7} M. In some experiments, the solvent used for the peptide was HF2P, in an attempt to reduce peptide self-aggregation and facilitate its incorporation into the bilayer. Finally, a few experiments were conducted in virtually solvent-free membranes, according to a technique derived from White (18) using squalene and pentane, but no significant differences were noticed. Voltage and current conventions are the usual ones: voltage is defined as positive if the more positive potential is applied on the side of peptide addition (*cis*-side), and positive current corresponds to cation transfer from this side to the opposite one.

Due to the peculiar ionophore properties of peptide 8(16-37)a and even, under certain conditions, of alamethicin (long-lived and mono-level open channels, to be described later), we performed control experiments with alamethicin for testing our set-up. The natural product (generous gift of Upjohn Co., Kalamazoo, MI, and of Professor G. Jung, Tübingen) is a mixture of several peptides (19) whose fraction 4, or R_F 30, was shown to induce resolved step-wise current fluctuations. Its isolation was conducted on a C 18 semi-preparative column (Waters Instruments, Inc., Rochester, MN) at a flow rate of 2 ml/min, the mobile phase being $EtOH/H_2O$ (65:35) and absorption detected at 210 nm.

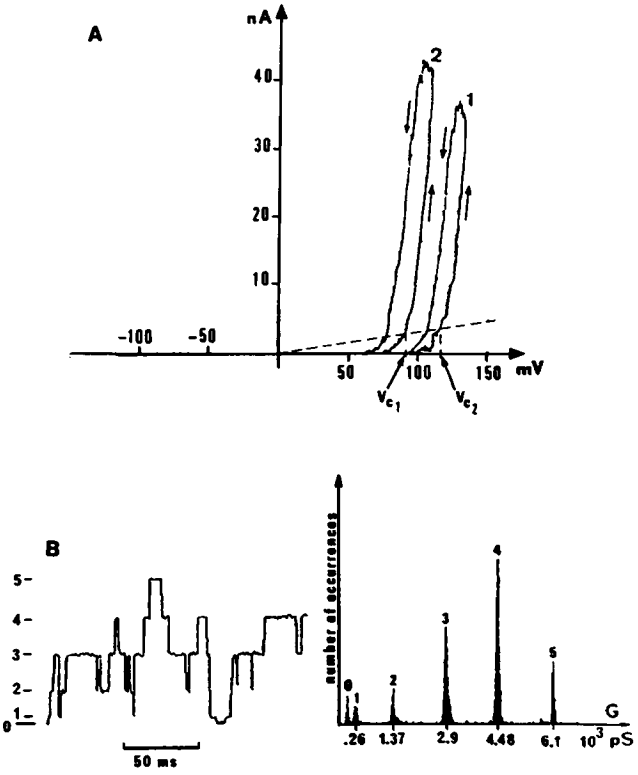

FIGURE 2 Controls, alamethicin-induced conductance. (*A*) Macroscopic current–voltage curves in a PE-decane membrane. The peptide concentration (*cis*-side) is $5 \cdot 10^{-8}$ M for curve *1* and 10^{-7} M for curve *2*. The dotted line represents a reference conductance of 3 nS. In this experiment, V_a (see text for definition) is 35 mV. (*B*) *Left*, single-channel current fluctuations; and *right*, the conductance amplitude histogram for an alamethicin concentration (*cis*-side) of $5 \cdot 10^{-9}$ M and a PE-decane membrane. Applied voltage: 140 mV; room temperature.

A macroscopic conductance ("many-channels") record in a phosphatidylethanolamine (PE)-decane membrane is shown in Fig. 2 *A*. For each concentration of alamethicin, a characteristic voltage V_c is defined (11) as the voltage for which the rising phase of the curve crosses a reference conductance level, chosen here as 3 nS. The concentration-dependence can be expressed by V_a, the shift of the characteristic voltage for an *e*-fold change in aqueous concentration and, similarly, V_c is the voltage that produces an *e*-fold change in conductance at a fixed peptide concentration. The mean values found in PE membranes are V_a = 54 mV and V_c = 5.5 mV. The corresponding figures in MMG membranes are 25.8 and 7.25 mV. Applying the analysis described by Hall et al. (11), the apparent number of monomers in a channel ($n = V_a/V_c$) was found to be respectively 10 and 4 (rounded values) in PE and MMG membranes. This latter value, although higher than previously published (11), remains in agreement with a geometric model derived by these same authors. A typical example of single-channel record with alamethicin in a PE membrane with the associated conductance amplitude histogram is presented in Fig 2 *B*. The usual sequence of substates is displayed and the mean values that we found for the amplitudes of the substates conductance (290, 1,330, 2,850, 4,450, and 6,200 pS, averaged from six experiments in 1 M KCl at room temperature) are in excellent agreement with the results of Hanke and Boheim (20).

RESULTS

Purification and Characterization of Both Peptides

The HPLC chromatogram of the non-acetylated peptide (Fig. 3 *A*, trace *a*) shows, apart from numerous small peaks, probably arising from the successive intermediate acetylations, two peaks (P_1 being a doublet and P_2) revealed towards the end of the gradient. Radio β-counting of the different collected and lyophilized peaks shows that only P_1 and P_2 are radioactive: 9,404 cpm/mg for P_1 and 10,328 cpm/mg for P_2, the expected value being 11,000 cpm/mg.

FAB mass spectrometry allowed an unambiguous differentiation of these products. The whole P_2 spectrum (Fig. 4 *A*) shows a molecular mass region between the 2,471.19 ($Cs_{10}I_9$) and 2,731 ($Cs_{11}I_{10}$) clusters. The enlarged spectrum (Fig. 4 *B*) gives an isotopic profile strictly similar to the one simulated on computer for the expected peptide 8(16-37) and allows the determination of the molecular mass M =2,624.5. The spectrum for P_1 discloses two regions that are at 16 and 32 mass units distant from the non-oxidized product P_2, indicating the existence of a mixture of sulfoxide for one of the two Met (at positions 20 or 34) with either the sulfoxide of the second Met or a sulfone. From the molecular mass ratio, the proportion of these two products can be estimated (single sulfoxide, 70%; and double sulfoxide or sulfone, 30%).

The acetylation of peptide 8(16-37) results in a translation on the chromatogram of the main peaks (doublet P'_1 and P'_2, Fig. 3 *A*, trace *b*) towards higher retention times. Radio β-counting (9,571 and 10,186 cpm/mg for P'_1 and P'_2, respectively, expected value 11,000 cpm/mg), and FAB mass determination confirms the presence of an acetylated and oxidized peptide as well as the acetylated and non-oxidized peptide 8(16-37)a (M = 2666.5).

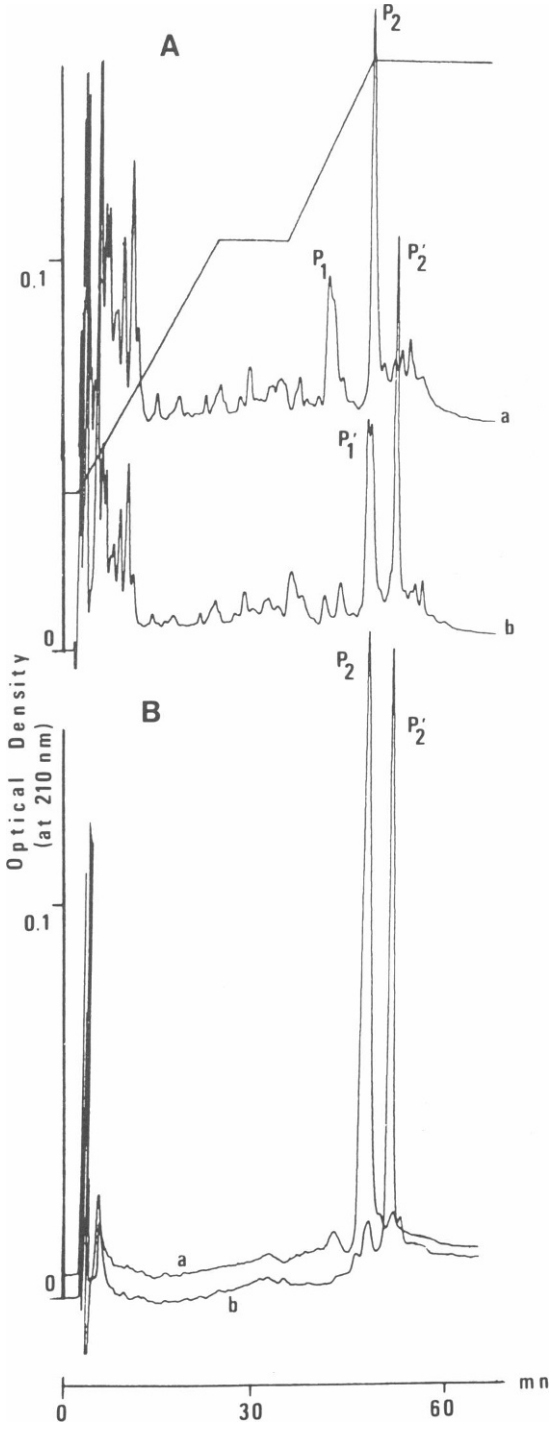

FIGURE 3 HPLC chromatograms of peptides 8(16-37) and 8(16-37)a on a RP 8 spheri 5 column (Brownlee Labs). Flow rates, 0.9 ml/min. Absorption monitored at 210 nm. Mobile phase: (*A*) EtOH/H_2O/TFA (50:50:0.05), (*B*) EtOH/H_2O/TFA (90:10:0.05). Upper traces show isocratic elution (5 min; *B*, 25%) followed by gradient (20 min; *B*, 62%), another isocratic elution (10 min; *B*, 62%), and then a new gradient (12 min; *B*, 88%) (*A*) Chromatograms of the raw products; trace *a*, peptide with free NH_2; trace *b*, acetylated products. Doublets P_1 and P'_1 for oxidized products; peaks P_2 and P'_2 for non-oxidized products. (*B*) Re-chromatograms of the collected fractions P_2 (non-acetylated peptide, trace *a*) and P'_2 (acetylated peptide 8(16-37)a, trace *b*). Same conditions and gradients as above.

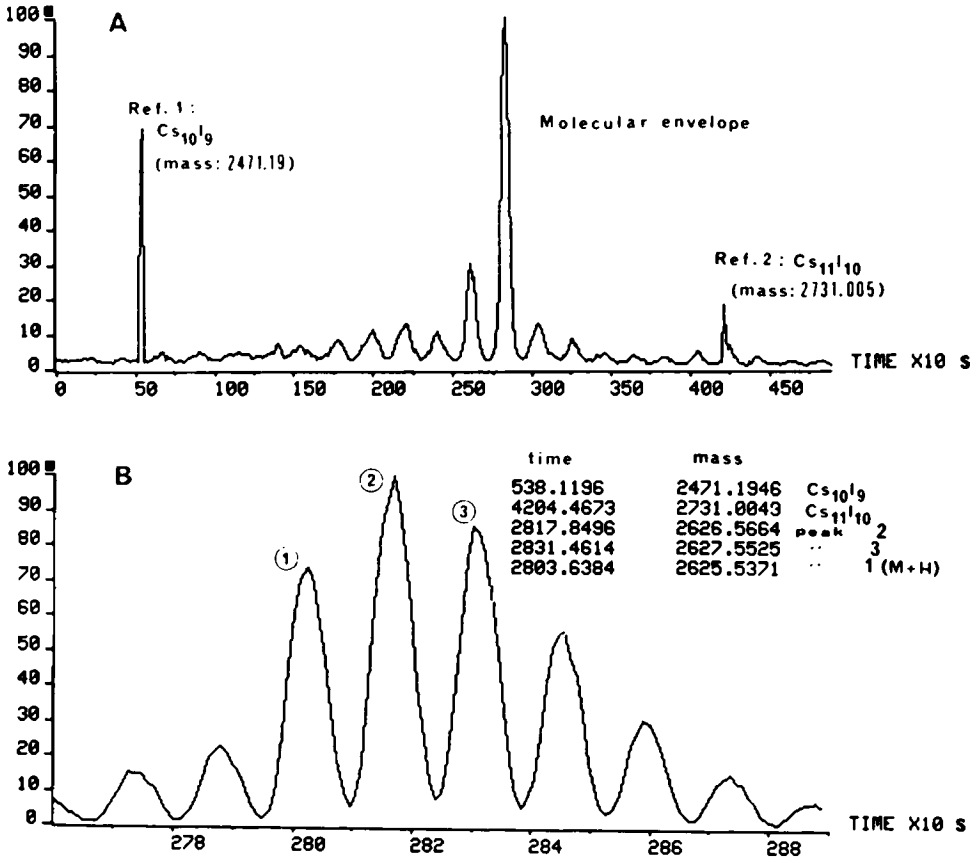

FIGURE 4 Positive FAB mass spectra for the nonacetylated peptide. The sample is dissolved in α-monothioglycerol. Voltage for ions acceleration, 8 KeV. Relative intensity as a function of time. (*A*) Whole spectrum calibrated with the two reference clusters; (*B*) detailed spectrum for the molecular region, the inset shows times and corresponding molecular masses for the product (peak *1*) together with peaks *2* and *3* corresponding to one and two ^{13}C isotopes.

The re-chromatograms of the purified products are shown in Fig. 3 *B*.

Conformational Studies

Although they differ only by the presence of an acetyl moiety on the NH_2 terminus, both peptides when examined under identical conditions reveal different spectroscopic characteristics. Infrared spectrum of the nonacetylated peptide 8(16-37) in the solid state shows an amide I band containing at least two components, at 1,653 and 1,626 cm^{-1}, while that of the acetylated derivative is well defined and lies at 1,655 cm^{-1} (Fig. 5), the amide II band being in both cases centered around 1,543 cm^{-1}.

For a poly-L-benzylglutamate α-helix chosen as a reference, these peaks are found at 1,655 and 1,547 cm^{-1}. These observations suggest that the acetylated peptide 8(16-37)a, at least in these conditions (dried MeOH or $CHCl_3$ film), adopts an α-helical conformation, while the non-acetylated product is built up of both α-helix and β-structure.

That conformational differences exist between the two peptides is corroborated by circular dichroism measurements (Fig. 6). When the products were dissolved in low dielectric constant solvents such as HF2P or in a HF2P-MeOH (1:1) mixture, the spectra indicate a higher α-helical content for the acetylated peptide. Even for the latter, however, the ellipticity is lower (60%) than that of a fully α-helical polypeptide, as could be expected owing to the presence of a Pro residue in position 33 (see Fig. 1 *A*), which disrupts the hydrogen bonding pattern of the α-helix.

Ionophore Properties and Comparison with Alamethicin

As mentioned in the Materials and Methods section, before the addition of any peptide the bare membrane silence was checked for 30 min with a series of voltage tests up to ± 200 mV.

The first trials with the non-acetylated peptide occasionally gave signs of channel activity either in the monoglycerides (MMG and MPG) or in PE membranes. Incorporation in the bilayer proved to be difficult and a basic pH was necessary to trigger a transitory activity. This was attributed to the positive charges at both ends of the molecule ($-NH_3^+$ at normal pH and Arg^+).

More successful results were obtained with the acetylated product to which the results below apply. In this case, due to the remaining formal charge (Arg^+ at the COOH terminus), it was expected that a negative voltage would be necessary to induce the conductance when the acetylated peptide was added to the *cis*-side. This prediction was supported by the observation that a negative voltage prevents gating in PE membranes of alamethicin, which

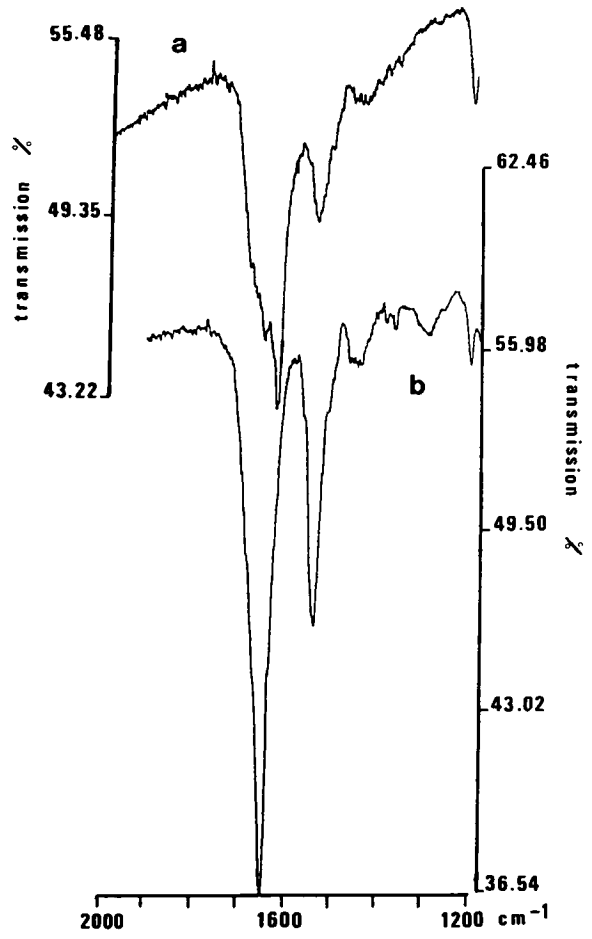

FIGURE 5 Infrared spectra restricted to the regions of amide I and amide II bands for the non-acetylated peptide (spectrum *a*) compared to the acetylated peptide (spectrum *b*). The transmission minimum is at 1,655 cm^{-1} (36.54%) for the amide I peak of the acetylated peptide, whereas the non-acetylated peptide gives two peaks at 1,653 and 1,626 cm^{-1}. In both cases, the amide II peaks are at 1,543 cm^{-1}.

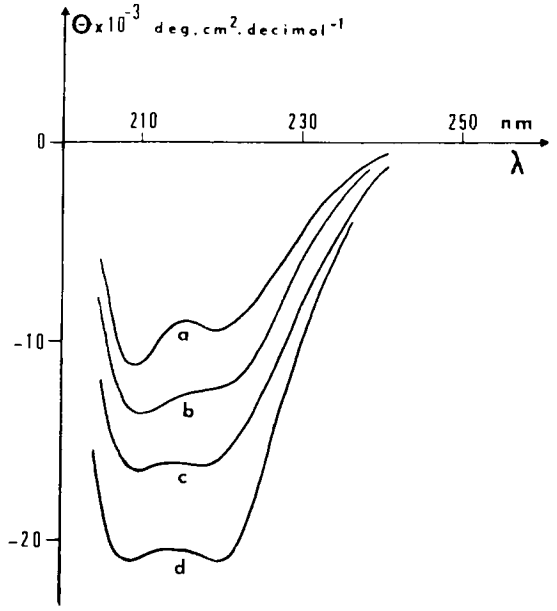

FIGURE 6 Circular dichroism spectra for the non-acetylated peptide: (*a*) in HF2P; (*b*) in HF2P-MeOH (1:1); and for the acetylated derivative (*c*) in HF2P and (*d*) in HF2P-MeOH (1:1).

has a negative charge at the COOH terminus that would probably anchor the molecule on the membrane surface.

The macroscopic current–voltage curves for the acetylated peptide in PE membranes (Fig. 7, *A* and *B*) show a voltage-dependent conductance increase in the negative quadrant when the peptide was added to the *cis*-side, in agreement with the above predictions. Part *A* of the figure also shows the concentration dependence of this branch which crosses, for the rising phase of the voltage cycle, a reference conductance of 3 nS at 194 and 161 mV ("characteristic voltages" V_{c1} and V_{c2}) for peptide concentrations of $2 \cdot 10^{-7}$ and $6 \cdot 10^{-7}$ M, respectively. Thus V_a, the V_c shift for an *e*-fold change in peptide concentration, is 30 mV. V_e, the voltage that produces an *e*-fold change of the conductance at constant peptide concentration, is 15 mV (for curve *2*). Thus, the apparent number of monomers in the channels $n = V_a/V_e = 2$.

As time elapses, the current–voltage curves in PE membranes evolve towards a smooth S-shaped form with a reduction of the asymmetry and hysteresis (Fig. 7 *B*). In MMG membranes, this latter kind of curve develops from the beginning of the experiment and is more symmetric (Fig. 7 *C*). For three increasing peptide concentrations, $1 \cdot 10^{-7}$, $2 \cdot 10^{-7}$, and $6 \cdot 10^{-7}$ M, the conductances at an absolute membrane potential of 150 mV, averaged for the positive and for the negative branches, are 5.1, 17, and 86.7 nS, respectively. The mean power dependence on peptide concentration is thus 1.6 (rounded value, 2). These results, very different from the alamethicin controls, are indicative of a weakly voltage-dependent conductance (V_e = 60 mV for $6 \cdot 10^{-7}$ M in MMG; Fig. 7 *C*).

As a rule, only one conductance level was observed in any given single-channel experiment. However, in a series of experiments there was a distribution of conductance levels, and two different and apparently independent states were observed in only two out of 38 experiments. The frequency of occurrences of the different states observed in MMG and PE membranes, with the average number of events per experiment, is shown in Table I. Out of a total 38 attempts in both membranes, 30 were successful, i.e., displayed at least one of the levels of Table I. Note that most of the negative attempts were with PE membranes. A minimum of 25 events was observed in at least one record for each level in a single lipid, except for the 1,200 pS level, which was of very long duration (~2s). Apparently, the MMG membranes allowed a wider distribution of states than in PE membranes. It should be stressed that, apart from only two experiments where two levels were recorded (see traces of Fig. 8, *A* and *D*), there was evidence for only one stable channel, belonging to one of the conductance states of Table I, fluctuating between one open state and the closed state.

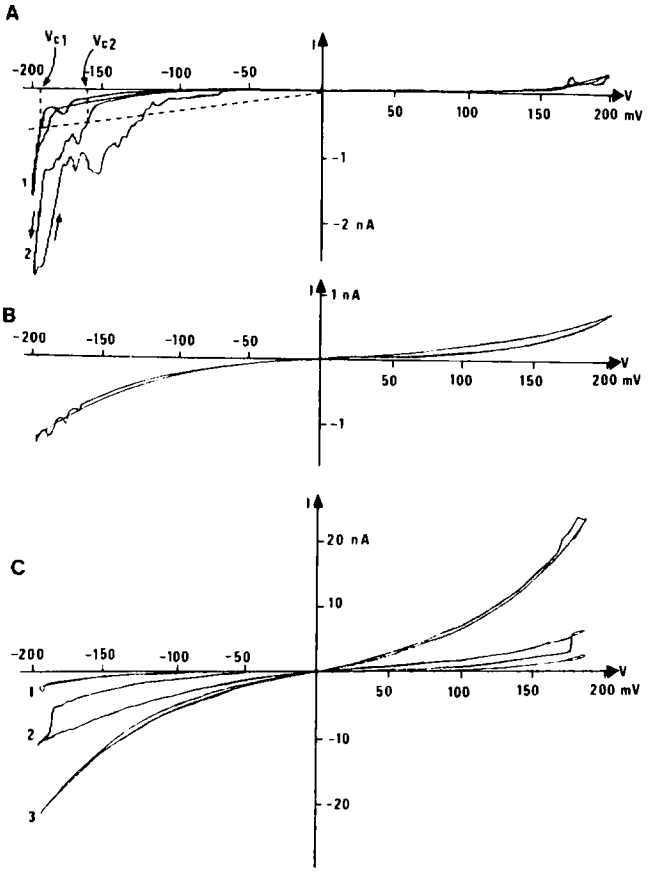

FIGURE 7 Macroscopic current–voltage curves induced by the peptide 8(16-37)a added to the *cis*-side. (*A*) In a PE-decane membrane at the beginning of an experiment. The dotted line represents a reference conductance of 3 nS. Curve *1* is for a peptide concentration of 10^{-7} M and curve *2* for $6 \cdot 10^{-7}$ M. The corresponding characteristic voltages V_{c1} and V_{c2} are 194 and 161 mV, respectively. (*B*) 30 min later in the same membrane (PE) for the latter concentration ($6 \cdot 10^{-7}$ M). (*C*) In MMG-decane membranes. The peptide concentrations are 10^{-7} M (curve *1*), $2 \cdot 10^{-7}$ M (curve *2*), and $6 \cdot 10^{-7}$ M (curve *3*).

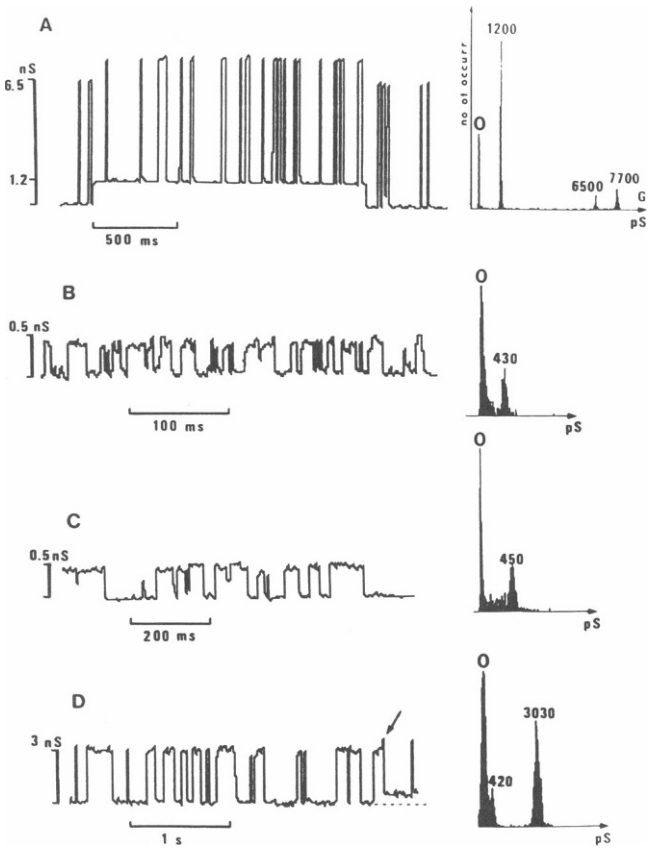

FIGURE 8 The different single-channel conductance states induced by the peptide 8(16-37)a in MMG-decane membranes. (*Left*) Examples of traces and (*right*) the associated amplitude histograms. (*A*) A high amplitude fluctuation (6,500 pS) of short duration apparently independent of a much longer level of 1,200 pS which was seen alone, earlier on in the same experiment. Membrane voltage, 75 mV and peptide concentration, 10^{-8} M. (*B* and *C*) A low conductance state of 430–450 pS recorded at two different membrane potentials (*B*, 200 mV; C, 130 mV) in the course of the same experiment. Peptide concentration, $2 \cdot 10^{-8}$ M. (*D*) In another experiment, a 3,000 pS level is disclosed. Note towards the end of the trace, the low level seen superimposed on the 3,000 pS level (*arrow*) and then alone. Membrane voltage, 35 mV and peptide concentration, 10^{-8} M.

The different situations encountered in MMG membranes, on which the study was focused because of the much higher probability of observing channels, are summarized in Fig. 8. The peptide was added to both sides of the membrane. Part *A* of the figure shows a high conductance level (6,500 pS) rapidly fluctuating and independent

TABLE I
FREQUENCY OF OCCURRENCES OF THE DIFFERENT CONDUCTANCE LEVELS INDUCED BY THE PEPTIDE 8(16-37)a IN MMG AND PE MEMBRANES

Conductance levels (pS)		80	440	1,200	3,000	6,500
Number of experiments in which they were observed	in MMG*	2 (18)	12 (22)	4 (10)	5 (12)	3 (26)
	in PE‡	—	3 (35)	—	3 (13)	—

In brackets: the average number of events per experiment.
*Out of a total of 27 attempts in MMG, 24 experiments were successful, i.e., displayed at least one of the above conductance levels.
‡In PE membranes, only six experiments out of 11 attempts were successful.
The 440- and 3,000-pS levels were observed together in only one experiment (in MMG) and both the 1,200 and 6,500 pS levels in another one (in MMG).

of the lower amplitude and longer duration level (1,200 pS), which was seen alone earlier on in the experiment. The fraction of time the higher level was opened was 0.10 compared with 0.70 for the lower level (at 75 mV). Another disclosed conductance level (430–450 pS) is shown in parts *B* and *C* of the figure for two different membrane potentials. The fraction of time this channel was opened was 0.38 (mean life-time, 10 ms) at 200 mV and 0.28 (mean life-time, 150 ms) at 130 mV. This weak voltage dependence is also illustrated in part *C* of the figure presenting another conductance level (3,000 pS) recorded for a membrane potential as low as 35 mV. Note towards the end of the trace the occurrence of the previously described lower level of 430 pS. Much more rarely a 80-pS level was recorded.

The strictly ohmic character of the unit conductances is demonstrated by the curves of Fig. 9 showing the single-channel current–voltage relations for the most frequently observed levels.

The above described ionophore properties of peptide 8(16-37)a are in contrast with the classical ionophore properties of alamethicin and recalled as controls at the end of the Materials and Methods section. Nevertheless, in MPG-decane membrane doped with alamethicin and at room temperature, very fast and unresolved (at this temperature) single-channel current fluctuations gave place, after 30–60 min, to events of unusual long duration and of constant amplitude in a given experiment, i.e., not fluctuating between substates. Out of 20 experiments, the most frequent levels were 5,300 pS (observed in five experiments, 197 events) and 2,700 pS (in 12 experiments, 138 events). More rarely, two other levels were also revealed: 3,900 and 1,600 pS. An example is shown in Fig. 10 together with the single-channel current–voltage relation. The fraction of time spent in the open 5,300 pS state is 0.93 (57 events) at 70 mV and 0.87 (52 events) at 30 mV, with mean lifetimes of 640 and 670 ms, respectively. This weak voltage-dependence and the fact that rather low voltages are sufficient to trigger this activity compares well with the behavior reported above for the peptide 8(16–37)a as does the distribution of states in a series of experiments.

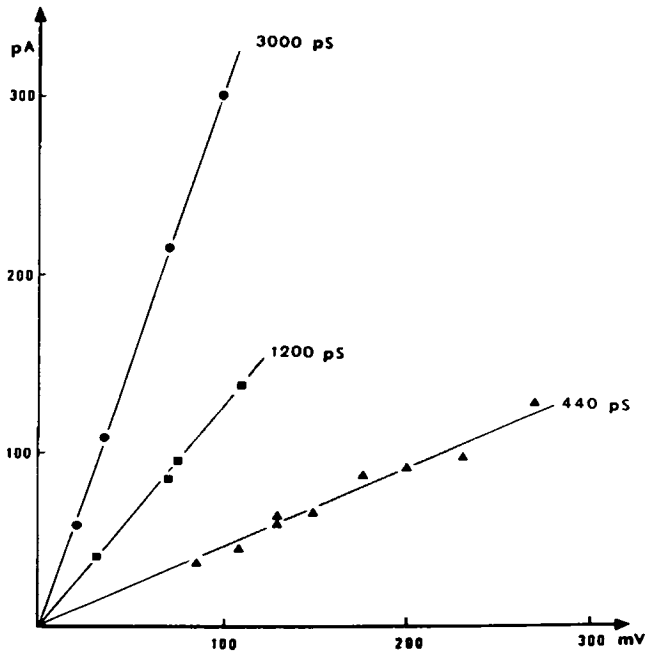

FIGURE 9 Single-channel current–voltage relations for the three most frequent channels induced by the peptide 8(16-37)a.

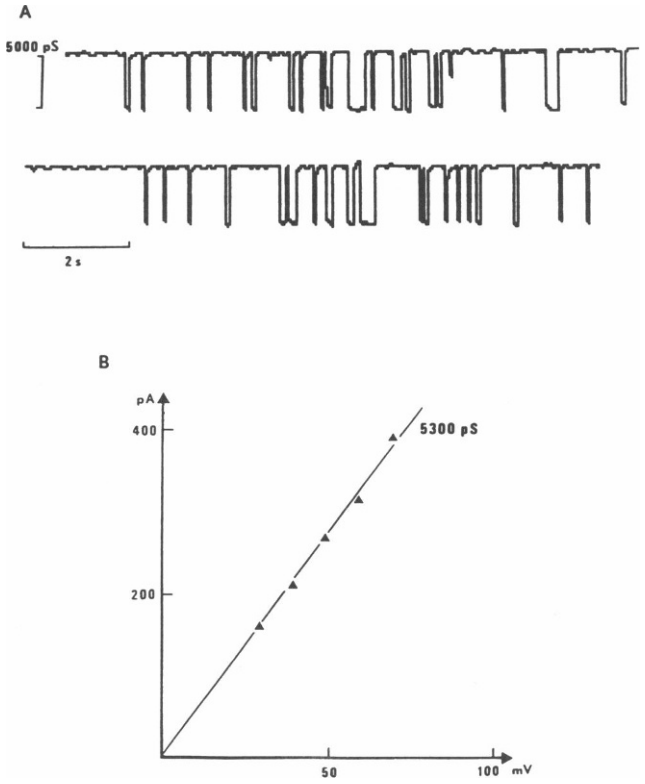

FIGURE 10 Long-lived channels of alamethicin ($2 \cdot 10^{-9}$ M) displaying only one single conductance level in MPG membranes. (*A*) Example of trace for the 5,300 pS level at a low membrane potential (30 mV). (*B*) Single-channel current–voltage relation for the 5,300 pS level. Triangles are mean values for 53 events at 30 mV, 37 at 40 mV, 35 at 50 mV, 18 at 60 mV, and 57 at 70 mV.

DISCUSSION

The synthesized acetylated peptide 8a(16-37)a, designed to reproduce the transmembrane fragment of subunit 8 of the F_o part of the H^+ ATP synthetase from *Saccharomyces cerevisiae*, behaves as an ionophore. The prevailing conformation for this peptide is the expected α-helix, as confirmed by the infrared and circular dichroism studies. The inspection of the α-helix projection, with its hydrophobic and hydrophilic sectors, led us to infer ionophore properties that could be similar to those of alamethicin, in particular, the fluctuations between single-channel conductance substates. The behavior in lipid bilayers of this well-studied peptide has been explained by various molecular models all

based on the "barrel-stave" arrangement of monomers, first proposed in 1974 (8, 9) and recently adapted (11) to account for the demonstration that no applied potential is required for the insertion of alamethicin into the bilayer (21). All these models consider an equilibrium between the monomers inserted at random in the membrane and aggregates of moderate size, up to about 10 monomers.

In the helix flip-flop model (22), the aggregates are built up of alamethicin dipoles arranged in antiparallel fashion. Under the application of an electric field, the monomers would rotate to a parallel configuration and, within an aggregate, neighboring dipoles then repel each other, creating a pore. Continual uptake and release of monomers would change the pore diameter and explain the fluctuation pattern of the single-channel conductance substates.

In another hypothesis, the transmembrane flip-flop is not necessary but rather the voltage-dependent step would be the ejection of a "core piece," i.e., a monomer not hydrogen-bonded to its neighbors (23).

A scheme developed recently (11) takes into account structural data derived from x-ray analysis and considers two steps triggered by the electric field change: a rotation of the dipole, crossing the membrane by its amino terminal, and a shift from β-sheet to α-helical structure for the COOH-terminal segment after Pro 14. In addition, this study (11) shows that the apparent number of monomers involved in the channels decreases with the membrane thickness.

All the models briefly reviewed above emphasize the strong voltage-dependence of alamethicin channels, as expressed by a steep exponential branch after a voltage threshold on the macroscopic current–voltage curves. However, for membranes doped with the peptide 8(16-37)a, the macroscopic conductance data suggest properties quite distinct from those of alamethicin. Indeed, when an exponential branch could be demonstrated initially (Fig. 7 *A*), the same analysis as for alamethicin gives an apparent number of only two monomers involved in the channels in PE membranes, which does not argue for a "barrel-stave" model. The evolution towards smooth S-shaped current–voltage curves (Fig. 7, *B* and *C*), with significant conductance at low voltage, points to a weakly voltage-dependent conductance and a peptide redistribution in the membrane. The macroscopic data are consistent with single-channel studies since the probability of opening for the most frequent channel (440 pS) is only slightly voltage-dependent and large conductance channels (3,000 pS) can be observed at low voltage.

According to these results, it seems that the peptide 8(16-37)a could adopt, at random, one state in a set of aggregate configurations and that transitions to other possible oligomeric states would then be forbidden. On the two occasions where two conductance levels were observed, there is evidence for two independent channels, and a notable feature is that the conductance fluctuations do not occur between two consecutive levels, for example between 440 and 1,200 pS or between 1,200 and 3,000 pS, but instead between 440 and 3,000 pS, the most probable levels, and also between 1,200 and 6,500 pS. This bypassing of one level could suggest the simultaneous incorporation of two monomers or rather of a dimer formed with two antiparallel helical rods. Nevertheless, the fact that a smaller (Fig. 8 *D*) as well as a larger (Fig. 8 *A*) conductance level can be superimposed on a previous level rules out any "respiration" of the channel through uptake or release of building units.

Likewise, in the case of the long-lived and mono-level channels of alamethicin reported here for the first time, the most frequently observed levels (2,700 and 5,300 pS) are separated by a rarer one (3,900 pS) in contrast with the binomial distribution of the usual multi-level channels of alamethicin. The increments between the levels are still increasing (1,100, 1,200, and 1,300 pS, from the lowest to the highest level) but when plotted, in double-log representation, as a function of $2n + 1$, n being the number of monomers building the pore in its different substates, no straight line of slope 1 could be demonstrated. This holds too for the peptide 8(16-37)a conductance increments. By contrast, this test of the circular "barrel-stave" model is positive in the case of usual multi-level channels of alamethicin (20, 24). Thus, for the mono-level channels reported here, the pore lumen need not necessarily be circular; slits between aligned rows of helical rods keeping a certain ionic selectivity could be envisaged.

The condition under which the long-lived and mono-level channels of alamethicin were observed (after a minimum of 30 mn in MPG at room temperature, but not in PE) support the idea of a redistribution or phase separation of the membrane components with alamethicin-rich domains, as already reported (25), and we propose that this process could be favored by a misfit between the membrane thickness and the length of the helical peptide. The difference between these two parameters has been found to be an important ingredient of a recent thermodynamic model, the so-called "mattress model" (26), designed to interpret experiments on the segregation of proteins in lipid bilayers. This redistribution would operate too for the peptide 8(16-37)a in thick (PE) as well as in thin (MMG) membranes. Indeed, its slighly longer helix could account for the fact that, in contrast with alamethicin, mono-level channels are observed also in PE membranes doped with the peptide 8(16-37)a, especially if one considers the part of the molecule between the NH_2 terminus and the proline near the COOH terminus: 17 residues, instead of 13 for alamethicin. Nevertheless, this hypothetical redistribution would be much less efficient or complete in thick than in thin membranes, as shown by the macroscopic conductance (for $6 \cdot 10^{-7}$ M and at 150 mV; 4.3 and 86 nS in PE and MMG membranes, respectively).

The finding of two similar single-channel conductance levels (440 and 3,000 pS) for the peptide 8(16-37)a, both in MMG and PE membranes, does not prove that the same

mechanism of association of helical rods is operating and, in particular, that the same number of monomers would be involved for each common conductance state in both membranes. In the normal behavior of alamethicin, the average number of monomers decreases from 10 in PE membranes to about four in MMG membranes (see the controls at the end of the Materials and Methods section and reference 11). Due to the shape of the macroscopic current–voltage curves displayed by the peptide 8(16-37)a, a similar systematic analysis as for the alamethicin controls could not be made, but the data suggest the same apparent number of monomers (2) for both MMG and PE membranes. Furthermore, if the same dependence in relation to membrane thickness as for the normal multi-level channels of alamethicin was at work in the case of the mono-level channels reported here, only low conductance levels should have been observed in thinner membranes. Table I shows that this was not the case. The second power dependence of macroscopic conductance on peptide 8(16-37)a suggest antiparallel dimers as the building units responsible for the weakly voltage-dependent conductance.

Contrasting with alamethicin, no transitory multi-level activity was ever observed with the peptide 8(16-37)a. This could be due to a quicker self-association or to large preformed aggregates since the mean hydrophobicity index (Table III in reference 27) for the α-helical part of peptide 8(16-37)a, between Pro 33 and Gly 16, is 0.82, as compared with 0.59 for alamethicin.

The behavior reported here may not be restricted only to the peptides 8(16-37)a and alamethicin but could also be shared by other amphiphilic peptides. In an initial phase, whose duration may depend on the relative thickness of the bilayer, on the length of the helical rods and on the hydrophobicity of the peptide, incorporation and release of monomers is allowed for small-sized aggregates (up to 10–12 monomers). Further enrichment and redistribution on both faces of the membranes and/or phase separation would bring about much larger aggregates or domains, whose inner pores would be isolated from the lipid phase by several layers of helical rods. This latter situation is reminiscent of the natural ionic channels, for example, the sodium channel is made up of 24–32 transmembrane segments (1, 2).

A recent study on aminoisobutyric analogues of alamethicin, as well as on alamethicin itself, reports long-lived events, in addition to the usual multi-level channels (28). We are presently undertaking a systematic study of the evolution of the single-channel conductance pattern of alamethicin, and preliminary results point to a gradual lengthening of the duration and to the stabilization of the most probable substates.

We thank S. Rebuffat (Laboratoire de Chimie du Museum d'Histoire Naturelle, Paris) for the purification of R_F30 fraction of natural alamethicin, kindly supplied by Upjohn Co. and by Professor G. Jung. We express our gratitude to the Service Central d'Analyses du CNRS in Lyon for mass determination (FAB spectroscopy) and to A. Van Dorsselaer (Centre de Neurochimie, Strasbourg) for isotopic profile computing and discussions, to the Centre CNRS-INSERM de Pharmacologie et d'Endocrinologie in Montpellier for access to the dichrograph, L. Maury for infrared spectrometry, and the Laboratoire d'Endocrinologie in Rouen for radioactivity measurements. We also thank Drs. O. S. Andersen and J. T. Durkin for reviewing the manuscript and for their helpful comments.

This work was supported by the CNRS AIP No. 6931.

Received for publication 22 October 1986 and in final form 16 June 1987.

REFERENCES

1. Noda, M., S. Shimizu, T. Tanabe, T. Takai, T. Kayano, T. Ikeda, H. Takahashi, H. Nakayama, Y. Kanaoka, N. Minamino, K. Kangawa, H. Matsuo, M. A. Raftery, T. Hirose, S. Inayama, H. Hayashida, T. Miyata, and S. Numa. 1984. Primary structure of *Electrophorus electricus* sodium channel deduced from cDNA sequence. *Nature (Lond.).* 312:121–127.
2. Greenblatt, R. E., Y. Blatt, and M. Montal. 1985. The structure of the voltage-sensitive sodium channel. *FEBS (Fed. Eur. Biochem. Soc.) Lett.* 193:125–134.
3. Ross, M. J., M. W. Klymkowsky, D. A. Agard, and R. M. Stroud. 1977. Structural studies of a membrane-bound acetylcholine receptor from *Torpedo californica*. *J. Mol. Biol.* 116:635–659.
4. Aslanian, D., T. Heidmann, M. Negrerie, and J. P. Changeux. 1983. Raman spectroscopy of acetylcholine receptor-rich membranes from *Torpedo marmorata* and of their isolated components. *FEBS (Fed. Eur. Biochem. Soc.) Lett.* 164:393–400.
5. Paul, D. L. 1986. Molecular cloning of cDNA for rat liver gap junction protein. *J. Cell Biol.* 103:123–134.
6. Kumar, N. M., and N. B. Gilula. 1986. Cloning and characterization of human and rat liver cDNAs coding for gap junction protein. *J. Cell Biol.* 103:767–776.
7. Unwin, N. 1986. Is there a common design for cell membrane channels? *Nature (Lond.).* 323:12–13.
8. Bauman, G., and P. Mueller. 1974. A molecular model of membrane excitability. *J. Supramol. Struct.* 2:538–557.
9. Boheim, G. 1974. Statistical analysis of alamethicin channels in black lipid membranes. *J. Membr. Biol.* 19:277–303.
10. Fox, R. O., and F. M. Richards. 1982. A voltage-gated ion channel model inferred from the crystal structure of alamethicin at 1.5-Å resolution. *Nature (Lond.).* 300:325–330.
11. Hall, J. E., I. Vodyanoy, T. M. Balasubramanian, and G. R. Marshall. 1984. Alamethicin: a rich model for channel behavior. *Biophys. J.* 45:233–247.
12. Velours, J., M. Esparza, J. Hoppe, W. Sebald, and B. Guerin. 1984. Amino acid sequence of a new mitochondrially synthesized proteolipid of the ATP synthase of *Saccharomyces cerevisiae*. *EMBO (Eur. Mol. Biol. Organ.) J.* 3:207–212.
13. Schindler, H., and N. Nelson. 1982. Proteolipid of adenosinetriphosphatase from yeast mitochondria forms proton-selective channels in planar lipid bilayers. *Biochemistry.* 21:5787–5794.
14. Spach, G., Y. Merle, and G. Molle. 1985. Peptides amphiphiles et canaux transmembranaires. *J. Chim. Phys.* 82:719–721.
15. Daumas, P., F. Heitz, J. Velours and B. Guerin. 1986. Transmembrane ion transfer induced by a new proteolipid of the mitochondrial H^+ ATP synthetase of *Saccharomyces cerevisiae*. *In* Forum Peptides Le Cap d'Agde. B. Castro and J. Martinez, editors. Les Impressions Dohr, Nancy. 109–111.
16. Merrifield, R. B. 1963. Solid phase peptide synthesis. I: The synthesis of a tetrapeptide. *J. Am. Chem. Soc.* 89:2149–2154.
17. Eisenberg, M., J. E. Hall, and C. A. Mead. 1973. The nature of the voltage-dependent conductance induced by alamethicin in black lipid membranes. *J. Membr. Biol.* 14:143–176.

18. White, S. H. 1978. Formation of "solvent free" black lipid bilayer membranes from glyceryl monooleate dispersed in squalene. *Biophys. J.* 23:337–347.
19. Vodyanoy, I., J. E. Hall, T. M. Balasubramanian, and G. R. Marshall. 1982. Two purified fractions of alamethicin have different conductance properties. *Biochim. Biophys. Acta.* 684:53–58.
20. Hanke, W., and G. Boheim. 1980. The lowest conductance state of the alamethicin pore. *Biochim. Biophys. Acta.* 596:456–462.
21. Quay, S. C., and R. Latorre. 1982. Molecular mechanisms of alamethicin channel gating. *Biophys. J.* 37:154–156.
22. Boheim, G., W. Hanke, and G. Jung. 1983. Alamethicin pore formation: voltage-dependent flip-flop of α-helix dipoles. *Biophys. Struct. Mech.* 9:181–191.
23. Mathew, M. K., and P. Balaram. 1983. A helix dipole model for alamethicin and related transmembrane channels. *FEBS (Fed. Eur. Biochem. Soc.) Lett.* 157:1–5.
24. Spach, G., F. Heitz, and Y. Trudelle. 1983. Peptides forming pores in bilayer membranes. *In* Physical Chemistry of Transmembrane Ion Motions. G. Spach, editor. Elsevier, Amsterdam. 375–383.
25. Mc Intosh, T. J., H. P. Ting-Beal, and G. Zampighi. 1982. Alamethicin-induced changes in lipid bilayer morphology. *Biochim. Biophys. Acta.* 685:51–60.
26. Mouritsen, O. G., and M. Bloom. 1984. Mattress model lipid-protein interactions in membranes. *Biophys. J.* 46:141–153.
27. Eisenberg, D. 1984. Three-dimensional structure of membrane and surface proteins. *Annu. Rev. Biochem.* 53:595–623.
28. Menestrina, G., K. P. Voges, G. Jung and G. Boheim. 1986. Voltage-dependent channel formation by rods of helical polypeptides. *J. Membr. Biol.* 93:111–132.